International Journal of Civil Engineering

Hydraulic Structure

Numerical simulation of acoustic cavitation in the reservoir and effects on dynamic response of concrete dams

R. Attarnejad[1,*], **F. Kalateh**[2]

Received: October 2009, Revised: February 2011, Accepted: May 2011

Abstract

This paper describes a numerical model and its finite element implementation that used to compute the cavitation effects on seismic behavior of concrete dam and reservoir systems. The system is composed of two sub-systems, namely, the reservoir and the dam. The water is considered as bilinear compressible and inviscid and the equation of motion of fluid domain is expressed in terms of the pressure variable alone. A bilinear state equation is used to model the pressure–density relationship of a cavitated fluid. A standard displacement finite element formulation is used for the structure. The Structural damping of the dam material and the radiation damping of the water and damping from foundation soil and banks have been incorporated in the analysis. The solution of the coupled system is accomplished by solving the two sub-systems separately with the interaction effects at the dam-reservoir interface enforced by a developed iterative scheme. The developed method is validated by testing it against problem for which, there is existing solution and the effects of cavitation on dynamic response of Konya gravity dam and Morrow Point arch dam subjected to the first 6 s of the May 1940 El-Centro, California earthquake, is considered. Obtained results show that impact forces caused by cavitation have a small effect on the dynamic response of dam-reservoir system.

Keywords: Dam–reservoir interaction; Finite element method; Nonlinear analysis; Cavitation; Concrete dams

1. Introduction

One of the nonlinear mechanisms in the dynamic response analysis of concrete dams that may occur during intense seismic excitation is formation and collapse of gaseous regions near the reservoir and dam surface due to cavitation. The collapsing of gaseous regions in the water would alter the hydrodynamic pressure acting along the upstream face of the dam and hence affect the dynamic response. In other words, a pressure wave propagating in a medium, interacting with a structure, produces cavitation. It is manifested by the separation of the medium from the structure at the interface. Such separation, i.e., cavitation, takes place because the structure-medium interface is unable to transmit a specific change in the pressure wave intensity. For example, if a pressure wave generated by an earthquake encounters a structure, a gap, (i.e. cavitation) may occur between the fluid and an interface normal to the direction of the compressive pressure wave propagation. In this case, the structure-fluid interaction results in a (tensile) excessive force at the interface that is not tolerated by the fluid and, therefore, a gap is produced. Cavitations continue until the gap closes, at which time, linear fluid-structure interaction is resumed.

Due to the complex nature of Cavitation, this phenomenon is not an extensively discussed topic in the dam-reservoir interaction. Nevertheless, for the rational vibration analysis of the dam-reservoir system, It is essential; in the evaluation of seismic response of concrete dams, the possibility of acoustic cavitation formation is considered. The dynamical behavior of coupled systems is characterized by different properties of the interacting subsystems that often describe different physical effects in the systems. However, high-performance algorithms have been developed for many special models; it is often inefficient to apply these algorithms to the entire systems. Therefore, in this paper attention is focused on the development of a new numerical procedure for computing the cavitating fluid effects on the dynamic response of the concrete arch dams. Although the main reason is to analysis the seismic response of dams, the proposed method is applicable to other fluid-structure systems in which the fluid is inviscid and undergoes small amplitude motion.

Several methods for analyzing the fluid-structure interaction

* *Corresponding Author: attarnjd@ut.ac.ir*
1 Faculty of Civil Engineering, School of Engineering, University of Tehran, P.O. Box 11365-4563, Tehran-Iran. Associate Professor
2 Faculty of Civil Engineering, School of Engineering, Ph.D. Candidate

have been developed. However, the most common approach is that both systems are coupled and solve as one system. For such coupled problems, formulations based on the displacement variables are generally chosen for the structure while the fluid is described by different variables such as displacement, pressure, potential function for displacement or velocity [1]. In the Eulerian approach, velocity potential, pressure or velocity is used to describe the behavior of the fluid. In the Lagrangian approach, the Finite Element mesh deforms with the fluid, and the response quantities both in the fluid and solid domains are the displacements of the finite element nodal points. Other methods include the arbitrary Lagrangian- Eulerian (ALE) method and the boundary element method (BEM). The ALE method attempts to take advantage of the strengths of both the Lagrangian and Eulerian approaches simultaneously. For example, in studying the seismic response of a dam, the Lagrangian approach would be used for the dam structure, while the ALE approach would be used for the reservoir. The difficulty in using an ALE technique for modeling fluid-structure problems is that it is still difficult to use this method for problems with complex geometries and complex interfaces [2]. The boundary element method is generally limited to linear problems, and usually requires the solution of a system of equations with an unsymmetric and unbounded matrix [3].

The possibility of acoustic cavitation forming in the dam's reservoir has been shown analytically and observed in model tests [4]. One analytical study of cavitation for a gravity dam monolith have been made by Clough and Chang [5], assuming incompressible water, showed that impact of the water resulting from collapse of the cavitation bubbles could increase tensile stresses in the top part of the dam by 20 to 40 percent. A more accurate representation of cavitation requires consideration of fluid compressibility, such as the bilinear constitutive model for cavitating inviscid fluid proposed by Bleich and Sandler [6] that presents a numerical treatment of cavitating fluids similar to smeared crack approach related to cracking propagation modeling. Zienkiewicz; et al. [7], used this fluid model to study the concrete dams and to clarify the phenomenon of cavitation; Zienkiewicz et al. distinguishes between the cavitation due to fluid flow and that due to elastic wave propagation. In the former, cavitation occurs due to the high flow velocity, which in turn reduces the absolute fluid pressure to below zero. This results in a periodic formation and the subsequent collapse of vapor bubbles in the high velocity region of the fluid domain. In the latter case, cavitation is attributed to the fluid expansion and often results in isolated regions of cavitation. The authors concluded that cavitation would not alter the maximum stresses of concrete gravity dam significantly. Due to these limited studies, the importance of cavitaiton in the earthquake response of concrete dams is still ambiguous. Specially, there has been no study of the cavitation effects on the concrete arch dams, where the dam-water interaction effects are more important than for the gravity dams [2]. In the literature, there are considerable disagreements on the importance of modeling the cavitation formation of reservoir in the studying of the seismic response of concrete dams.

Various numerical methods have been employed to simulate the cavitation phenomenon in the liquid using finite element method (a detailed description can be found in Ref.[2] and [8]). These methods can be categorized into four main classes; 1) Using pressure based finite element formulation for the fluid domain and the displacement base FEM for the structure domain. 2) Applying displacement base FEM for both fluid and structure domains. 3) Representing the fluid response in terms of a potential function for displacement or velocity and using the displacement base FEM for the structure domain. 4) Another approach for computing the response of fluid-structure coupled system involves a combination of the formulations mentioned above. A major problem that arises when modeling inviscid fluids using a displacement based Lagrangian formulation is that due to the absence of shear stresses, spurious zero energy modes may contaminate the numerical results. Such problems have been reported in the past by various researchers using a displacement based Lagrangian formulation for the modeling of the fluid continuum in fluid-structure interaction problems. To eliminate zero energy modes, several stabilization methods have been proposed [9], such as the introducing of artificial stiffness and the enhanced strain method. Felippa and DeRuntz [10] also employed a displacement potential finite element fluid formulation to study the Bleich –Sandler problem. The latter method was developed by Sprague and Geers [11] with their cavitating acoustic spectral element (CASE) formulation. Sandberg [12] used the pressure and density as independent nodal variables in the finite element formulation. Rose and et al. [13] presented a new coupling method, based on the localized Lagrange multiplier (LLM) method, for studying the interaction of an acoustic fluid with flexible structure and used a displacement potential formulation for modeling the cavitating fluid.

From the literature review carried out above, the way of modeling the cavitation phenomenon at the fluid-structure interfaces seems to be an important and developing subject. The question of whether the cavitation is important for simulating a realistic response of arch dams will be addressed in this study. Therefore, a special program has been developed for calculating the modified hydrodynamic pressure that acts along upstream face of dam, due to cavitation in the reservoir. In the developed method, a pressure based and a displacement based finite element formulation has been used, for modeling the fluid and solid domains, respectively. Following the work of Sandberg [12] we have developed a modified method for modeling the cavitation effects in dam's reservoir base on the improvement the stiffness matrix of the cavitated fluid finite element, implemented it into a substructure model configuration of fluid-solid interaction, and used a staggered method to solve the equation of motion. By applying this solution method, we can solve the equation of motion of each field separately at each time step and force interaction effects through their interface and avoid assembling matrices with a large bandwidth. This saves the required memory, especially for the cases with non-symmetric matrices. In the present work, the equation of motion governing the fluid is expressed in terms of pressure alone considering the fluid as compressible, inviscid and irrotational. Comparative studies show clearly the efficiency and effectiveness of the proposed method. The system under consideration, which is shown in Fig. 1, consists of a structure domain and a fluid domain with their common interface and other five surface boundaries.

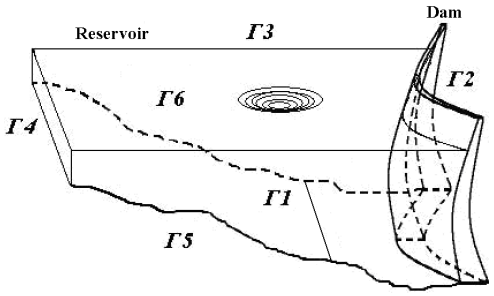

Fig. 1. Dam-reservoir system and definition of reservoir boundaries

2. Governing Equations for the fluid medium

The general governing equations for a compressible and viscous fluid can be written as

Continuity equation:

$$\frac{\partial \rho}{\partial t}+\frac{\partial(\rho_0 u_i)}{\partial x_i}=0 \tag{1}$$

Momentum Equation:

$$\frac{\partial(\rho_0 u_i)}{\partial t}+\frac{\partial(\rho_0 u_i \cdot u_j)}{\partial x_j}=-\frac{\partial P}{\partial x_i}+\frac{\partial \tau_{ij}}{\partial x_j} \tag{2}$$

$$\tau_{ij}=\mu\left(\frac{\partial u_i}{\partial x_j}+\frac{\partial u_j}{\partial x_i}\right) \tag{3}$$

And the Equation Of state (EOS):

$$P=f(\rho,\dot{\rho})=\alpha(\rho)\cdot\rho+\beta(\rho)\cdot\frac{\partial \rho}{\partial t} \tag{4}$$

In the present work, the momentum equation is simplified to represent an inviscid fluid that undergoes small amplitude and irrotational:

$$\rho_0\frac{\partial u_i}{\partial t}+\frac{\partial P}{\partial x_i}=0 \quad \text{or} \quad \rho_0\frac{\partial u_i}{\partial t}+\nabla P=0 \tag{5}$$

where ρ, P, ui, μ are density, pressure, velocity and viscosity of the fluid, respectively, and x_i is the spatial coordinate in the ith direction. ρ_0 is the reference value of the fluid density and f is an arbitrary ,nonlinear function of ρ and $\delta\rho/\delta t$ By differentiating Eq. (1) with respect to time and eliminating the velocity field, we can write:

$$\nabla^2 P=\frac{\partial^2 \rho}{\partial t^2}. \tag{6}$$

It should be noted that, a constant pressure-density relationship is adequate for modeling non-cavitating fluids such that $P=C_w^2.\rho$. However, for a cavitating fluid the pressure density relationship changes as the fluid alternates between a cavitating and a non-cavitating state and vice versa, that leads to a nonlinear equation of acoustic pressure wave propagation (see Eq. 6). By substituting Eq. (4) (with assuming $\beta(\rho)=0$) into Eq. (6), this Equation is simplified to

$$\nabla^2 P=\frac{1}{\alpha(\rho)}\frac{\partial^2 P}{\partial t^2} \quad (\text{or} \quad \alpha(\rho)\cdot\nabla^2 P=\frac{\partial^2 P}{\partial t^2}) \tag{7}$$

Where, $\alpha(\rho)$ can be defined as follows:

$$\begin{cases}\alpha(\rho)=C_w^2 & \text{when } \rho \geq -P_s/C_w^2\\ \alpha(\rho)=-P_s/\rho & \text{when } \rho \leq -P_s/C_w^2\end{cases} \tag{8}$$

Equation (8) shows a bilinear relationship between pressure and density of a fluid that is specified by the acoustic pressure wave propagation in the fluid elements. If the absolute pressure of each fluid domain element is above the vapor pressure of the fluid, $-P_s$, then it is assumed that the velocity of the acoustic pressure wave C_w is equal to the velocity of sound in the water and if the absolute pressure drops below $-P_{ss}$ thus it is assumed that C_w becomes close to zero.

3. Boundary Conditions of Fluid Domain

For the 3D dam's reservoir, there exist six boundaries; therefore, we can define the hydrodynamic aspects completely if the appropriate boundary conditions are applied on these boundary surfaces. Below, we represent the boundary conditions that are used in this work for the fluid medium.

3.1. Far End Boundary of Reservoir

The specification of the far-boundary condition at the truncation surface has been presented elaborately in Maity and Bhattacharyya [14]. The far-boundary condition adopted in the present case is:

$$\frac{\partial P}{\partial n}=-\frac{1}{\sqrt{\alpha(\rho)}}\cdot\frac{\partial P}{\partial t} \tag{9}$$

Where, n is the normal at the truncation boundary and $\alpha(\rho)$ is defined in Eq. (8), in other words, $\alpha(\rho)$ is the velocity of sound in the fluid with linear behavior. Different far end truncation boundary conditions for the finite element modeling of infinite reservoir were introduced by researchers. As a rule for the truncation boundary, there is no reflection for the outgoing wave and all the efforts are made for modeling the energy loss in outgoing wave such that all of the energy can be absorbed on the truncation boundaries. Here, we have assumed that the hydrodynamic waves can be considered as plan waves, which lead to the one dimensional wave propagation equation (9). This represents well-known Sommerfeld radiation condition. It introduces some damping in the system and models the loss of energy in the outgoing waves. This boundary condition performs well in time domain analysis when it is applied sufficiently far from the structure and it is applicable only if compressibility is included [15].

3.2. Reservoir Boundaries Absorption

The energy loss capability of the reservoir bottom materials is approximately modeled by a boundary condition for the reservoir bottom and banks as follow:

$$\frac{\partial P}{\partial n}=-\frac{1}{\beta\cdot\sqrt{\alpha(\rho)}}\frac{\partial P}{\partial t} \tag{10}$$

This energy loss is represented by the damping coefficient q, which is related to the wave reflection coefficient α by

$$\lambda = \frac{1-q\sqrt{\alpha}}{1+q\sqrt{\alpha}} = \frac{1-\dfrac{\rho\sqrt{\alpha}}{\rho_s C_s}}{1+\dfrac{\rho\sqrt{\alpha}}{\rho_s C_s}} = 1/\beta \tag{11}$$

Where $\alpha(\rho)$ is defined in Eq. (8) and ρ is the density of water. ρ_s and C_s are the density and sound velocity for the bottom materials, respectively. β is the acoustic impedance ratio of rock to water, n, is the normal vector to the boundary. It should be noted that on the banks boundaries of the reservoir we apply similar condition but with different acoustic impedance ratio based on materials property of the banks.

3.3. Free surface boundary condition

Considering the effects of surface waves of the fluid, the boundary condition of the free surface is taken as:

$$\frac{\partial P}{\partial n} = -\frac{1}{g}\cdot\frac{\partial^2 P}{\partial t^2} \tag{12}$$

where g is gravity acceleration and n is the normal direction outward into the boundary surfaces. At the surface of a fluid, relatively large vertical motions are possible. Pure sloshing motion does not involve volume change within the fluid. The physical behavior of these modes involves fluctuation in the potential energy of the fluid at the surface. In addition, the kinetic energy exists due to both the vertical and horizontal velocity of the fluid.

3.4. Fluid-Structure Interface Condition

Considering the dam to vibrate with an acceleration of $\ddot{u}_g(t)$ the condition along the dam-reservoir interface may be specified as:

$$\frac{\partial P}{\partial n} = -\rho_{fluid}\cdot\left(\ddot{u}_g + \ddot{u}_a\right)_n = -\rho_{fluid}\cdot\left(\ddot{u}_{total}\right)_n \tag{13}$$

where P is the hydrodynamic pressure, ρ is the density of water and n is normal to the interface and its direction as well as its value at a point are constant. $\ddot{u}_a$ is the nodal acceleration produced by the flexible dam and $\ddot{u}_g$ is the ground acceleration . At the interface of fluid-structure, it is clear that there must not be any flow across the interface. This is because of the fact that the surface of the concrete dam is impermeable. This leads to the condition that, there is no relative velocity at the normal direction to the boundary. In other words, the velocity of the structure and fluid along the normal direction into interface boundary is equal.

4. Cavitation modeling

The development of an efficient numerical algorithm for simulating the cavitated fluid has remained a challenge in scientific computation. One of the difficulties is that the complex cavitating process is still not well understood. Therefore, a general cavitating models that takes into account all features and physical aspects of phase transition is not available. Typical analysis provides the normal compatibility and tangential slip at the fluid/solid interface, but do not separate the fluid from the solid if the fluid pressure drops to a tensile or negative value. Many researchers have proposed different cavitation models. Among these models, the homogeneous equilibrium model (HEM) and the transport equation model (TEM) are most commonly used ones. In the HEM, some kind constitutive equation is needed to provide the relation between the density and other properties. Since most of cavitating processes are considered to be isothermal, many researchers use a barotropic equation of state (EOS), $P=f(\rho)$ to describe the pressure-density relation [16]. However, by assuming the pressure as only a function of density, some physics may be lost. Significant progress has been achieved recently in the development of homogeneous mixture models for the simulation of three-dimensional transient cavitating fluid. These models allow single-fluid solvers to be applied to the conservation equations.

In the present work, in order to model the effect of cavitation, as mentioned earlier (see Eq. (8)), we use a bilinear equation of state proposed by Bleich and Sandler [6].by applying this model two methods have been presented in the literatures. Both methods utilize a bilinear relationship and note that during the process of cavitation the compressibility and bulk modulus of water are reduced to zero,(see Fig. 2), where p is the pressure, p_v is the vapor pressure, K is the bulk modulus of the fluid, ρ_0 is the density of the saturated liquid, and ρ is the instantaneous density. Thus, the first model utilizes the fact that the inception of cavitation is associated with a local sudden drop in the tangent water compressibility and therefore modifies the fluid stiffness [17]. The second model utilizes the fact that the pressure of the cavitation region has changed and makes the appropriate corrections through the pressure term [10-12].

In this study we apply the first method in the analysis process (Fluid Stiffness modification method). When the total pressure in a fluid element drops below the vapor pressure, then the stiffness matrix is modified to suppress rigidity of the element. In other words, if the total pressure of the element is found to be less than the vapor pressure, then the global stiffness matrix of the fluid domain can be modified by assembling the stiffness matrices of the fluid elements, which have been already calculated. However, to reduce the computational cost during time step, it is best to determine the cavitation effect of each element on the stiffness matrix of the fluid element during preprocessing phase. Then, if the element is found to be in the cavitation region, the matrix of cavitated fluid element is modified appropriately. As previously mentioned, modification of the constitutive properties during cavitation is

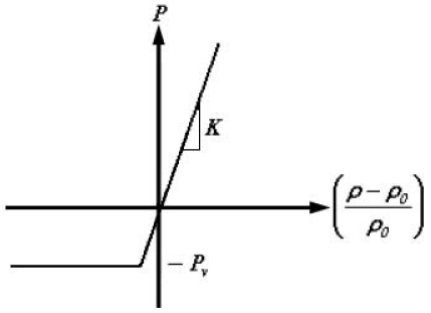

Fig. 2. Bilinear equation of state for fluid

similar to the crack smearing approaches for tensile crack growth in concrete [18]. After the cavitation region has formed, it is possible that the earthquake direction will change, this causes the micro bubbles region created by cavitation to collapse and the cavitation region close up again. Because of the sudden closure of the fluid cavities, an impact on the dam will occur [17]. This impact phenomena results in a sharp increase in compressive pressure that followed by spurious oscillations [19]. To eliminate these high frequency oscillations several authors [10-12] have added a small amount of numerical damping. Others, [17-18] have added a small amount of damping to the water domain in their analysis. The small amount of damping that required to remove the spurious oscillations has been found to have a small effect on the response of the system [17].In present work, we use a stiffness proportional damping to remove the high frequency oscillations caused by frothing. The mass proportional term has been omitted because it would provide some artificial numerical instability during the time marching process. [18]

5. Finite Element discretization of Nonlinear Fluid Equation

The weak form of Eq. (7), employing Green's theorem, yields

$$\int w \cdot \ddot{P}\, d\Omega + \int \nabla w \cdot \alpha(\rho) \nabla P\, d\Omega = \int w \cdot \alpha(\rho) \frac{\partial P}{\partial n} d\Gamma \tag{14}$$

The surface integral in the RHS of Eq. (14) can be used to apply various boundary conditions on the reservoir boundaries that will be discussed in the next section. Expanding p in terms of a set of shape functions, $\{N_i\}$

$$P = \sum_j N_f^j \cdot P_j \tag{15}$$

Where P_j is the unknown value of P at node j. In the present study, as noted earlier, numerical damping is necessary to suppress spurious oscillations, therefore, a stiffness proportional damping adds to the formulation as follow:

$$\underbrace{\left[\int N_f^i N_f^j \, d\Omega\right]}_{[G_{ij}]}\ddot{P} + \underbrace{\left[\eta \int \nabla N_f^i \nabla N_f^j \alpha(\rho) d\Omega\right]}_{[D_{ij}]}\dot{P} + \underbrace{\left[\int \nabla N_f^i \nabla N_f^j \alpha(\rho) d\Omega\right]}_{[H_{ij}]}P = \underbrace{\int w\alpha(\rho)\frac{\partial P}{\partial n} d\Gamma}_{[L_{ij}]} \tag{16}$$

Where Ω denotes the fluid domain, Γ is fluid domain boundaries and n is the outward normal vector along boundary and η is the coefficient of fluid Stiffness proportional damping that added into formulation for suppressing spurious oscillations, finally, the discretized form of Eq. (7) can be written as follow:

$$\begin{cases} [G]\cdot\{\ddot{P}\} + [D]\cdot\{\dot{P}\} + [H]\cdot\{P\} = -\Phi[Q]\{\ddot{u}_a + \ddot{u}_g\}_n \\ \Phi = \rho_f \cdot \alpha(\rho) \end{cases} \tag{17}$$

Where $\{P\}$ represents the vector of nodal pressures for water domain. ρ_f is density of water , [Q] is coupling matrix that will be introduced in the section 7 and $\{\ddot{u}_a + \ddot{u}_g\}_n$ is the vector of total acceleration of fluid-structure interface in the normal direction. [G], [D] and [H] are quasi-mass, damping and stiffness matrix of fluid medium that may be defined as follow:

$$\left.\begin{aligned} [G] &= \sum \int_{\Omega} [N]^T [N] d\Omega + \sum \int_{\Gamma_f} \frac{\alpha^e}{g} [N]^T [N] d\Gamma \\ [D] &= \sum \int_{\Omega} \eta \alpha^e \left(\frac{\partial}{\partial x}[N]^T \frac{\partial}{\partial x}[N] + \frac{\partial}{\partial y}[N]^T \frac{\partial}{\partial y}[N] + \frac{\partial}{\partial z}[N]^T \frac{\partial}{\partial z}[N] \right) d\Omega + \\ &\quad \sum_{\Gamma_t} \sqrt{\alpha^e} [N]^T [N] d\Gamma + \sum_{\Gamma_b} \frac{\sqrt{\alpha^e}}{\beta_b} [N]^T [N] d\Gamma + \sum_{\Gamma_{rb}} \frac{\sqrt{\alpha^e}}{\beta_r} [N]^T [N] d\Gamma + \\ &\quad \sum_{\Gamma_{lb}} \frac{\sqrt{\alpha^e}}{\beta_l} [N]^T [N] d\Gamma \\ [H] &= \sum \int_{\Omega} \alpha^e \left(\frac{\partial}{\partial x}[N]^T \frac{\partial}{\partial x}[N] + \frac{\partial}{\partial y}[N]^T \frac{\partial}{\partial y}[N] + \frac{\partial}{\partial z}[N]^T \frac{\partial}{\partial z}[N] \right) d\Omega \\ [Q] &= \sum_{\Gamma_s} \alpha^e [N]^T n [N] d\Gamma \end{aligned}\right\} \tag{17}$$

Where α^e is defined in Eq. (8) and β_b, β_r, β_l are the acoustic impedance ratio of the bottom of the reservoir materiel, right-bank material and left-bank material to water, respectively, that takes to account partial absorption form perimeter of reservoir. The subscripts *f, s, b, rb, lb* and *t* represent the free surface, solid-fluid interface, reservoir bottom, the right bank of the reservoir, the left bank of the reservoir and truncation boundary, respectively.

6. Governing equations for solid

Applying standard procedure for the finite element discretization of the structural domain, the equations of motion for the structure subjected to ground motion can be represented by the following:

$$[M]\{\ddot{U}\} + [C]\{\dot{U}\} + [K]\{U\} = -[M]\{\ddot{u}_g\} + \{F_{Coupling\ Force}\} \tag{17}$$

Where [M], [C] and [K] are mass, damping and stiffness global matrices of solid domain and $\{\ddot{u}_g\}$ is the ground acceleration applied on the base of dam structure and $\{F_{Coupling\ Force}\}$ hydrodynamic force along upstream face of the dam structure resulting from adjacent fluid. The equation of motion of structure domain employs a Newmark scheme for discretisation. The Newmark scheme is one of the most popular algorithms in structural dynamics. Because of Methods of dynamic analysis of structures are well established and will not be discussed in this study.

7. Solution algorithm

Coupling across fields can be complicated because different fields may be solving for different types of analysis during a simulation but the coupling between the fields can be accomplished by either direct or load transfer coupling. In a fluid-structure interaction problem the fluid pressure causes the structure to deform, which in turn causes the fluid solution to change. This problem requires iterations between the two physics fields for convergence. In this study, we introduce a coupling matrix [*Q*] that relates the pressure of the reservoir and the forces along the dam-reservoir interface as follow:

$$[Q]+\{P\}=\{F\} \tag{20}$$

Where [*Q*] is coupling matrix and *P* is Hydrodynamic pressure vector acting on interface and *F* is the force vector acting on the structure due to the hydrodynamic pressure. Fig. 3. shows an

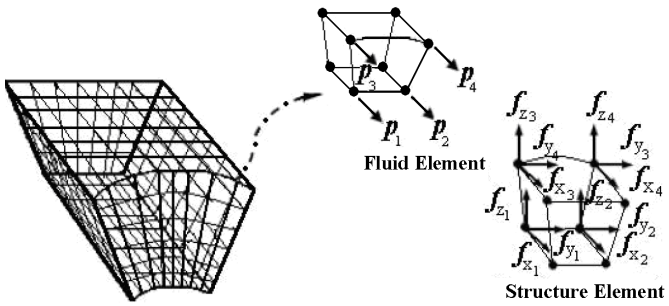

Fig. 3. Interface element on the dam-reservoir interaction boundary

element on the interaction boundary of the dam-reservoir. The work done by the hydrodynamic pressure on the interaction surface of the structure must be equal to the work of the equivalent nodal forces on the interface boundary of an element [20]. With applying this hypothesis can get a relation equation for coupling matrix [Q] as follow:

$$[Q]^e = \int_{\Gamma_e} \{N_S\} n \{N_f\}^T d\Gamma \tag{21}$$

Where N_s is the structure shape function and N_f is the fluid shape function and n is the normal vector on interface. In the present study, eight node brick elements for pressure and twenty node brick elements for displacement have been adopted for solution of Eq. (19) with the prescribed boundary conditions. The dam structure is analyzed by 3D solid formulation having on side reservoir. A stabilized staggering iterative scheme has been developed to achieve the coupled effect of dam-reservoir system. At any instant of time t, the resulting hydrodynamic pressure and cavitation forming is evaluated by solving the fluid domain using Eq. (17) with appropriate boundary conditions. At the same time instant, the developed pressures exerts forces on the adjacent structure, as the hydrodynamic forces are the function of generated pressure, the dam is analyzed with the forces, developed due to hydrodynamic pressures, using Eq. (19). The application of staggered solution methods in coupled problems is more obvious, however, this solution methods is only conditionally stable [20-21], so that , the stability limit is indeed the same as if a fully explicit scheme were chosen for the fluid phase[22-23]. For this reason, we apply the stabilization scheme in the staggered displacement method in our solution process; proposed procedure can be summarized by following steps:

- Solve following equation and calculate $\{\ddot{u}^*\}^{n+1}$:

$$[M]\{\ddot{U}^*\}^{n+1} = \{F_1\}^{n+1} + [Q]\{P\}^{n+1} - [C]\{\dot{U}\}^{n+1} - [K]\{U\}^{n+1} \tag{22}$$

- Substituting $\{\ddot{u}^*\}^{n+1}$ in the following equation and solve for $\{\mathrm{P}\}^{n+1}$

$$\left([G] + \rho_f \beta \cdot \Delta t^2 [Q]^T [M]^{-1} [Q]\right)\{\ddot{P}\}^{n+1} + [D]\{\dot{U}\}^{n+1} + [H]\{U\} = -\rho_f [Q]^T \{U^*\}^{n+1} \tag{23}$$

- Substituting $\{\mathrm{P}\}^{n+1}$ in below equation to calculate $\{\ddot{u}^*\}^{n+1}$ and its derivatives.

$$[M]\{\ddot{U}\}^{n+1} + [C]\{\dot{U}\}^{n+1} + [K]\{U\}^{n+1} = \{F_1\}^{n+1} + [Q]\{P\}^{n+1} \tag{24}$$

Where $\{U\}$ is the displacement vector and [M],[C],[K] are mass, damping and stiffness global matrices of structure domain and $\{F_1\}$ is external load vector at current time step and $\{Q\}$ is coupling matrix and $\{P\}$ is Hydrodynamic pressure vector at current time step and [G],[D],[H] are quasi mass, quasi damping and quasi stiffness matrix of fluid domain and β is parameter of the Newmark time-integration method . The Proposed solution algorithm is shown in Fig. 4. Due to the additional Hydrodynamic force that acts along upstream face of dam, the dam undergoes a displacement. As a result the dam-reservoir interface boundary changes and hence the solution of the water domain. The water domain is solved again at the same time instant with the changed conditions of displaced structure boundary and a check for cavitating elements was made in the following manner and applied appropriate modification in cavitated fluid stiffness element. If any new cavitated fluid element is found, then fluid domain reanalysis and this process repeat until at the current time instant no new cavitated element is found and satisfy some convergence criterion.

$$\left(P_{Hydrodynamic\ Pressure} + P_{Hydrostatic\ Pressure} + P_{atm}\right)_{Center\ Of\ i^{th}\ Element} \le 0$$
$$\Downarrow \tag{24}$$
Element is Cavitated

Consequently, the structural system is also analyzed with changed forces. Thus, at time t, both the hydrodynamic pressure $\{p\}_t$ and the structural displacement $\{u\}_t$ are iterated simultaneously until a desired level of convergence is achieved. Thus,

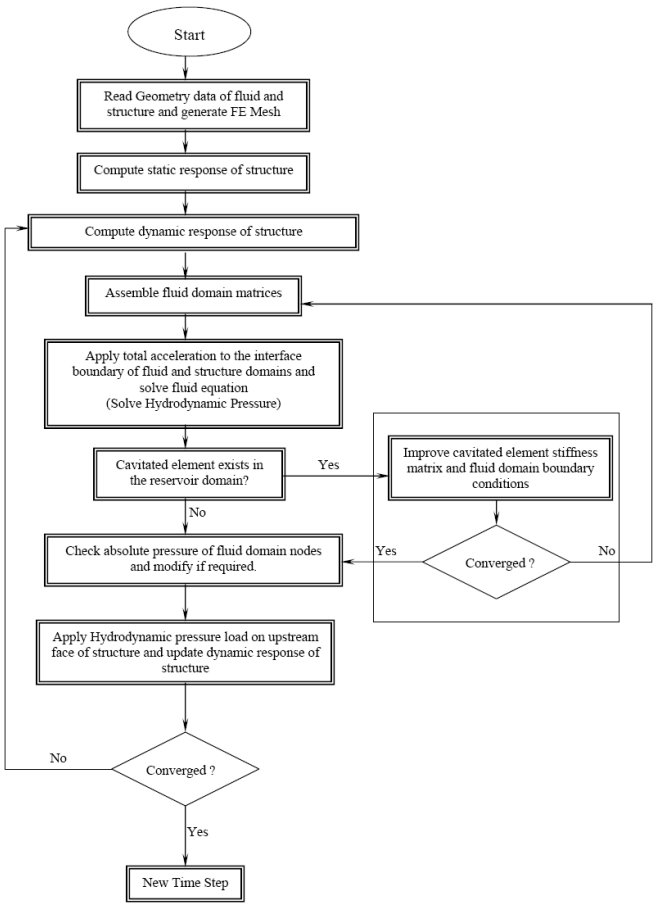

Fig. 4. Solution algorithm.

$$\frac{\left\|\Delta p_t^i\right\|}{p_{max}} \le tol_{Euclidean} \text{ and } \frac{\left\|\Delta u_t^i\right\|}{u_{max}} \le tol_{Euclidean} \quad (26)$$

i being the number of iteration; $\|\Delta u^i_t\|$, $\|\Delta p^i_t\|$ are the Euclidean norm of the displacement and pressure for ith iteration, respectively, u^{max}, p^{max} are maximum displacement and pressure achieved current iteration, respectively, $tol_{Euclidean}$ is a small preassigned tolerance value, In which, assumed 10^{-3} in thus study. The most costly operation involve in this algorithm is successively solve nonlinear equation of fluid system and linear equation of structure system at each iteration. But in the present case, matrices involve in the solution of the system of equations of solid domain are saved in a skyline manner and decomposed into triangular forms at the beginning of the iteration and thereby only two forward-eliminations and back-substitutions are required at each iteration step.

9. Validation and Application

A computer code was developed to compute the dynamic response of dam-reservoir systems due to caviation forming in the reservoir in the basis of above-mentioned algorithm. The performance and characteristics of the developed program are evaluated in this section. The developed program use the 8 node fluid elements for discretization fluid domain and 20 node elements for modeling structure domain and we provide a mesh generation subroutine in the program for generate finite element mesh of fluid and structure medium. In order to examine the feasibility and the accuracy of the proposed algorithm and demonstrate cavitation effects on dynamic response of arch concrete dams, several examples are presented and results are compared with those based on other work.

9.1. Example 1:

First, a benchmark problem has been solved and compared with the existing literature. The idealized three-dimensional fluid-structure system considered is shown in Fig. 5, this system comprised of a semi-infinite fluid filled impermeable cylinder that confined with a solid cap in one of its end and truncated with a transmitting boundary in other end. Radiation boundary is located at the end of the *270 m* long fluid domain. The structure has a mass of *857 ton* and the Poisson's ratio and the modulus of elasticity of structure are *0.2* and $E_s=2.3\times10^6$ *ton/m²*, respectively. Dimension of structure and fluid domain and corresponding finite element meshes are shown in Fig. 6. For the fluid, $\rho_0=1$ *ton/m³* and $C_w=1440$ *m/sec* are density and sound speed in the water, respectively. The ground motion is idealized by a sinusoidal ground acceleration with a peak value of $a=0.31g$ and an excitation frequency equal to *21 rad/sec*. This problem is a three-dimensional version of that was considered in Ref.1 and is included here for comparison. We use finite element model to analysis the problem. In the first finite element model of coupled system, fluid domain

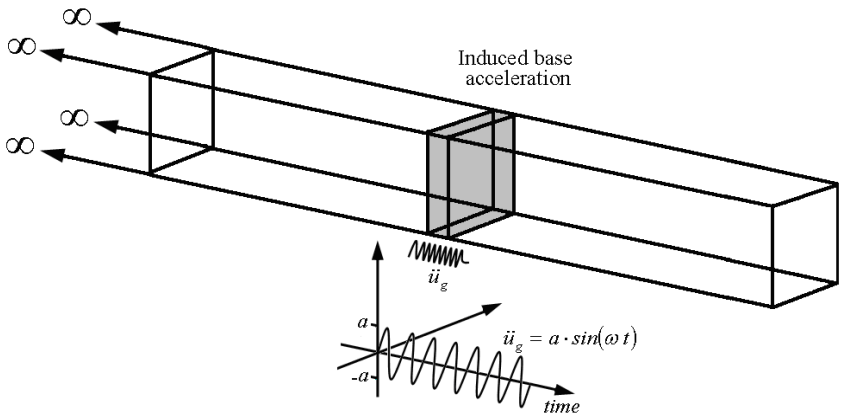

Fig. 5. Three-dimensional fluid-structure system subjected to harmonic motion.

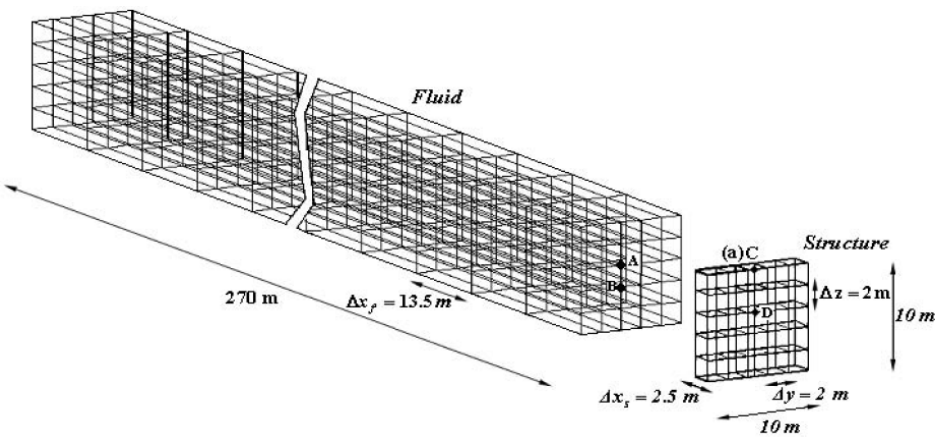

Fig. 6. Definition of finite element fluid and structure model and key dimensions.

consisted of 500 eight-noded fluid elements, with 36-interface fluid node and the structure domain is discretized using 25 twenty-noded finite elements, with 96-interface structure node. The equations of motion are solved using the fully implicit time-integration method and a time step of $\Delta t=0.01sec$ is used. The above parameters are equivalent to those used by Fenves et. al. [1] to validate the proposed cavitation formulation. A small amount of artificial damping is included in the fluid to eliminate high frequency spurious oscillation form numerical solution. Corresponding results are shown in Fig. 7.

Cavitating region create in the near of fluid-structure interface when the motion of structure in the downstream direction cause fluid and structure separate each other and fluid pressure fall into below of vapor pressure of fluid. As the structure change direction, the cavitated region collapses and form larger peak pressures at higher frequencies than if a linear fluid is assumed. Applying of cavitation effect in fluid-structure model results in larger displacement in downstream direction but generally reduces the displacement in the upstream direction. In the overall, good agreement between all sets of results is demonstrate. The discrepancy between the numerical results may be attributed to the use of different dimensional descriptions of problem and some assumption in the solution process and boundary conditions.

9.2. Example 2: Cavitation effects on the response of shock wave impact on a floating structure

To verify the analysis procedure, benchmark test is performed. This example consists of a floating structure that subjected to a step exponential plan wave. This example is one-dimensional Bleich- Sandler problem [6], this test case is often referred to in literature, because it has been solved analytically and validated by many other researchers [7-10]. The structure is modeled using five 20-node brick element while water under the structure is modeled by 100, 8-node fluid volume elements as is shown in Fig. 8. The depth of the fluid is 3.81 m. The peak pressure, P_0, is 0.710 MPa and the decay time,θ is 0.9958 *ms*. The density and sound speed of the fluid in this case are 1000 kg/m^3 and 1450 *m/s*, respectively. The atmospheric pressure is 10.3 ton/m^2. These material properties and parameters are identical to those used in the papers published by Sprague and Geers [11]. Fig. 9 illustrates the velocity history of the floating structure center for both cases of with and without cavitation, which matches well with Bleich-Sandler analytic solution [6].

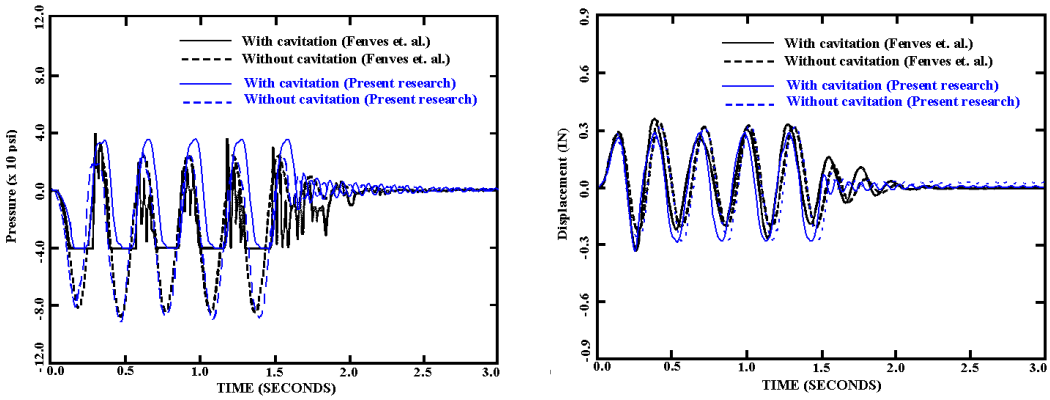

Fig. 7. Response of fluid-structure system to harmonic excitation, (piston problem).

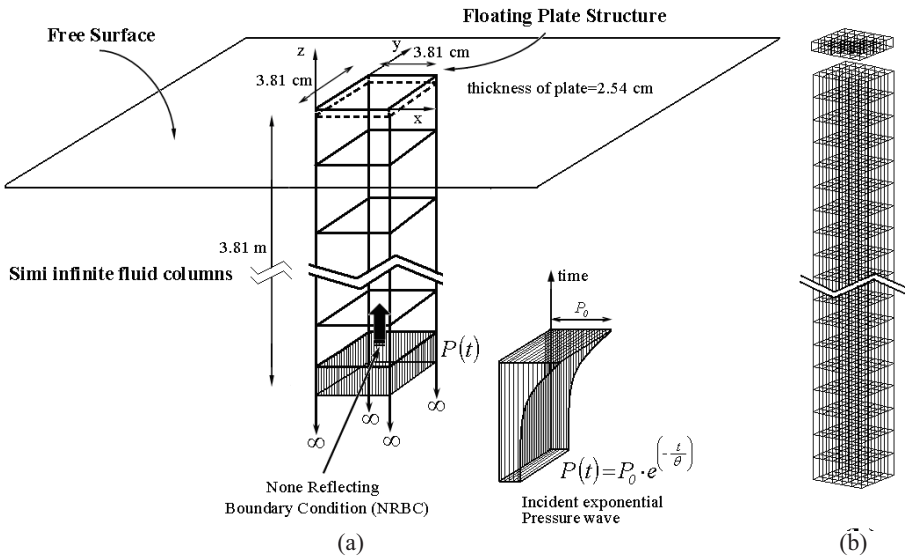

Fig. 8. a) One-dimensional of the cavitation model implementation with the bleich and sandler problem. b) Finite element model

9.3. Example 3: Cavitation effects on dynamic response of a gravity dam

The objective of this example is to assess the accuracy and performance of the proposed formulation for fluid-structure interaction problems with the reservoir cavitation effects on the seismic response of the Koyna gravity concrete dam that is investigated and compared with the results have been previously obtained by M. R. Ross [13]. Konya Dam in India is a 103 m high concrete gravity dam which Built over 1954-1963, was damaged by a Richter magnitude 6.5 a strong reservoir-induced earthquake that generated in the dam a peak acceleration of approximately 0.5g. Fig. 10 shows the geometry and dimensions of the dam and the reservoir. Physical parameters chosen for the coupled system are as follows. For the dam concrete: $E_c=3.146\times106$ *ton/m²,* $v_c=0.2$ and $\rho_c=2.69$ *ton/m²* For the reservoir water: $C_w=1439$ *m/s* and $\rho_w=1.019$ *kg/m³*

The 1940 El Centro earthquake is chosen as input. Acceleration records of the NS component are shown in Fig. 11. The horizontal excitation normal to the dam is taken to be the NS Component. Fig.10. shows a representative coarse and refined FE model of the coupled system that uses to analysis of dynamic response of gravity dam. In order to validate the coupling solution scheme, without consideration of cavitation, a comparison is accomplished between time history of crest displacement of Koyna dam that is presented in Ref. [24] and computed in the present research, as is shown in Fig. 12, good agreement is seen between numerical results.

Damping plays an important role in dynamic analysis. In this example, Rayleigh damping is used. The first and the fifth fundamental frequencies are used to determine the values of the

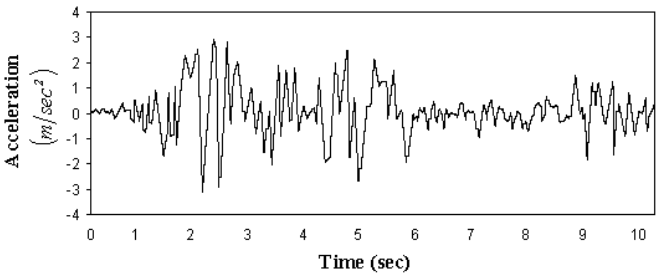

Fig. 11. Ground acceleration due to El centro earthquake 1940

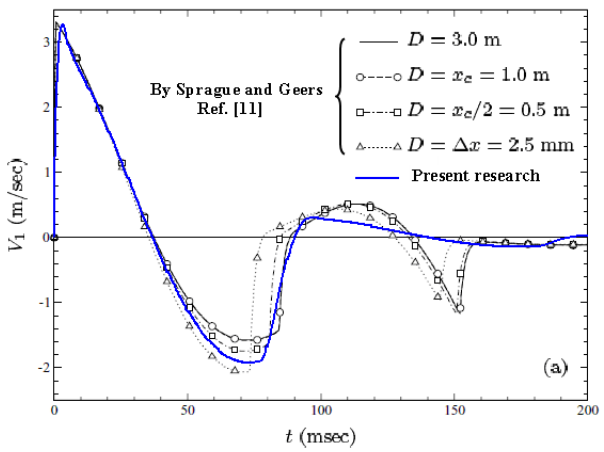

Fig. 9. Velocity response history of a floating structure subjected to a shock wave –effects of cavitation

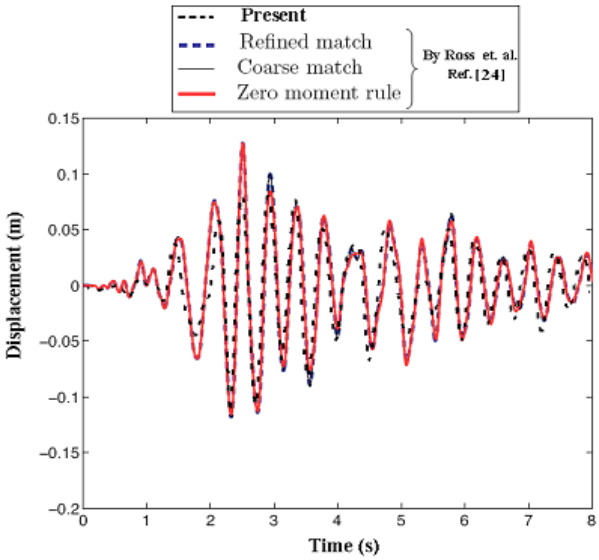

Fig. 12. Comparsion of time history of dam crest displacement of Koyna gravity dam subjected to El-Centro earthquake, presented in Ref. [24] and present research. (maximum of peak acceleration is 0.32g)

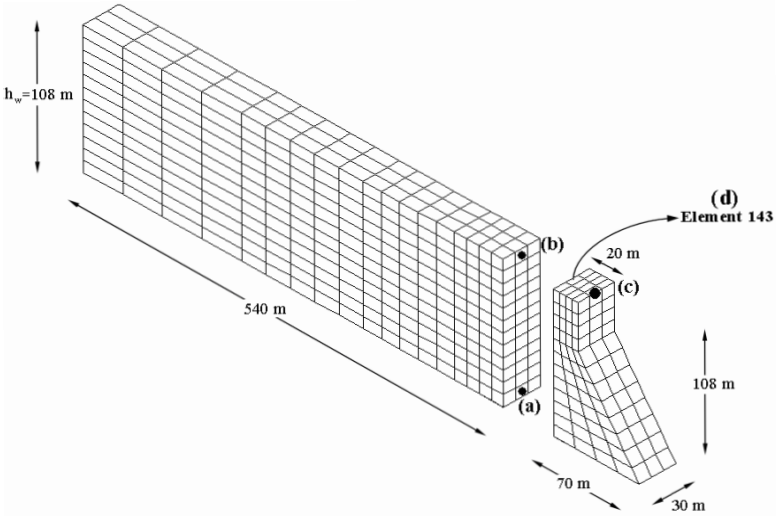

Fig. 10. Finite element model of koyna gravity dam- reservoir system and corresponding dimensions

mass and stiffness coefficients that would produce a damping of 5% in both modes. Medina [25] indicated that if effective length of fluid element has been chosen smaller than the one fourth of the smallest hydrodynamic pressure wave length the results have been proper accuracy, in this respect, we use $\Delta x = 13.5\ m$ in the reservoir FE mesh ,therefore a Δt of 0.01 sec is sufficient for accurate response of the model with cavitated fluid. An initial static analysis is undertaken to determine the values of the displacements and stresses due to the hydrostatic and the weight of the structure. These values are considered as the starting conditions of the dynamic run. The response of the dam to the applied ground motion is shown in Fig. 13 that is computed using coarse and refined FE meshes. In the coarse mesh, we use 380, 8-node fluid elements and 80, 20-node brick elements to modeling fluid-structure system and in the refined mesh; we apply 680, 8-node fluid element and 160, 20-node brick elements to discretizing coupled dam-reservoir system. The location of far end boundary of the reservoir domain is chosen through the sensitivity analysis that is indicated assuming reservoir length equal to 300 m form upstream face of dam is sufficient and utilizes larger length has any effect on the dam's response. Obtained results are indicated that the response of dam is independent of the numerical mesh chosen in the simulation.

In Fig. 14, the effect of cavitation on the response of Konya

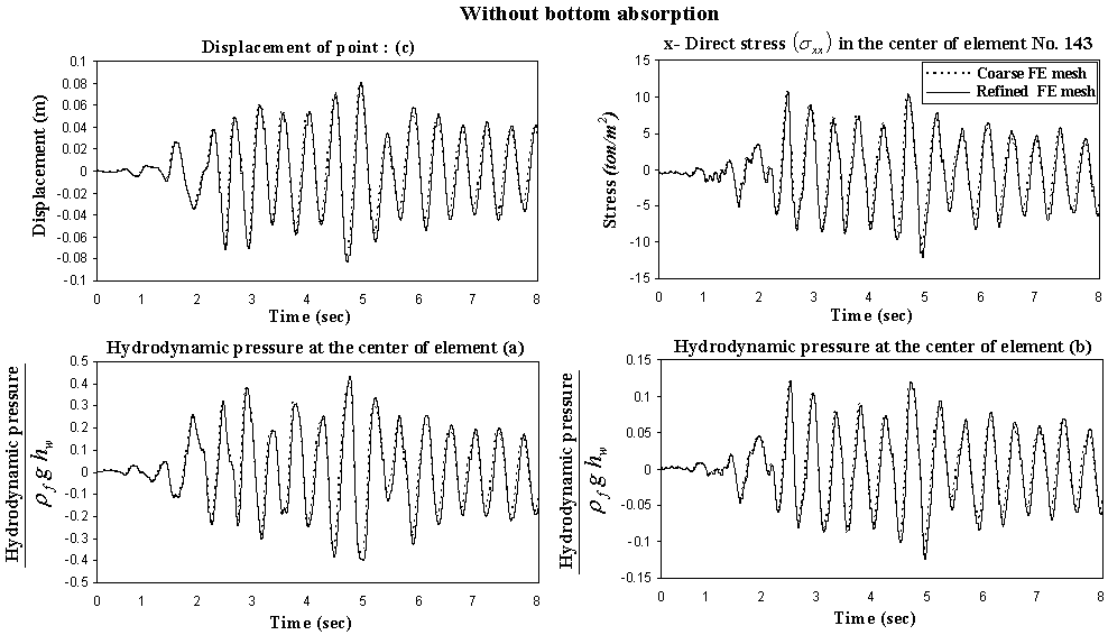

Fig. 13. Comparison of koyna gravity dam dynamic response subjected to horizontal component of EL-centro earthquake for coarse and refined FE meshes.

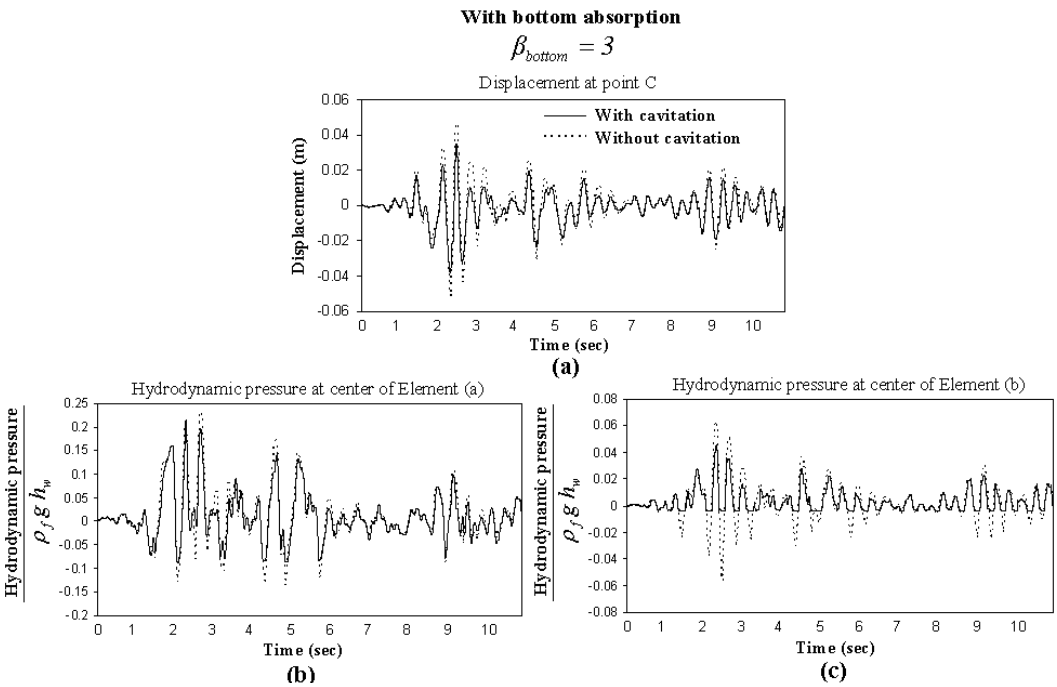

Fig. 14. Response of konya gravity dam to horizontal component of El-centro earthquake; peak acceleration is 0.32 g. (refined FE mesh).

gravity dam is investigated using refined FE model. The hydrodynamic pressure-time variation in the nodal points A and B of the reservoir mesh on the interface are depicted Figs. 14(c) and 14(d). It is clear that the hydrodynamic pressure greatly affected by the cavitation formation, obtained results indicate that the peak of hydrodynamic pressure reduces due to cavitation.

Nevertheless, there is a large amount of cavitation in the water; the effect on maximum displacement and stresses in the dam is small and cavitation reduces the response of dam, as shown in Fig. 14. Cutoff of negative pressure reduces the upstream hydrodynamic force on the dam, at the upper part of dam, reducing the magnitude of the displacement and stresses expect some peak response because of cavitated region collapsing. Obviously, the earthquake response of Konya gravity dam is small affected by nonlinear behavior of the water due to cavitation.

The stress contours given in Fig. 15, at three different time station, *t=2.5 sec*, *t=5.0 sec, t=7.0 sec* for with and without considering cavitation, indicated that the resulting stresses are smaller than those computed with ignoring cavitation effects. Cavitation zones in the reservoir behave similar isolation layer between dam and reservoir that cause dynamic pressure wave act on upstream face of dam partially. Table 1, presents the maximum stress values at the center of two different dam's element that create in the dam body during El-Centro earthquake.

Evolution of the cavitation zone over six second time span is shown using the proposed method in Fig.16 with adding a stiffness proportional artificial damping equal to *0.0005* that included in the reservoir formulation. As is shown in Fig. 11 cavitation due to fluid expansion results in isolated regions of cavitation and fragmentized cavitating zones in the reservoir.

A comparison of the results show a good agreement in the obtained results form present study and others [1-7-13]. The some discrepancy between the results may be attributed to the use of different dimensional definition of problem and different boundary condition on the reservoir boundaries. For instance, in the latter example, we consider the absorption of the pressure wave through sedimentary material deposited on the reservoir bottom with applying $\beta_{bottom}=3$ that alleviates the response of dam.

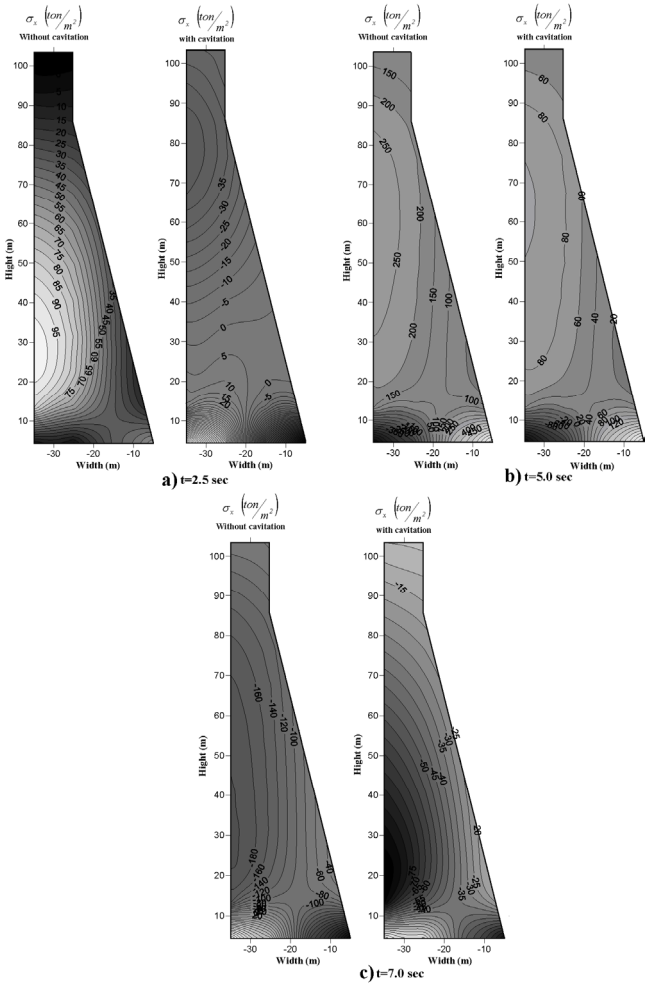

Fig. 15. Extremes of σ_{xx} due to dynamic response of koyna gravity dam to El-centro ground motion (Peak acceleration scaled to 1.0 g)

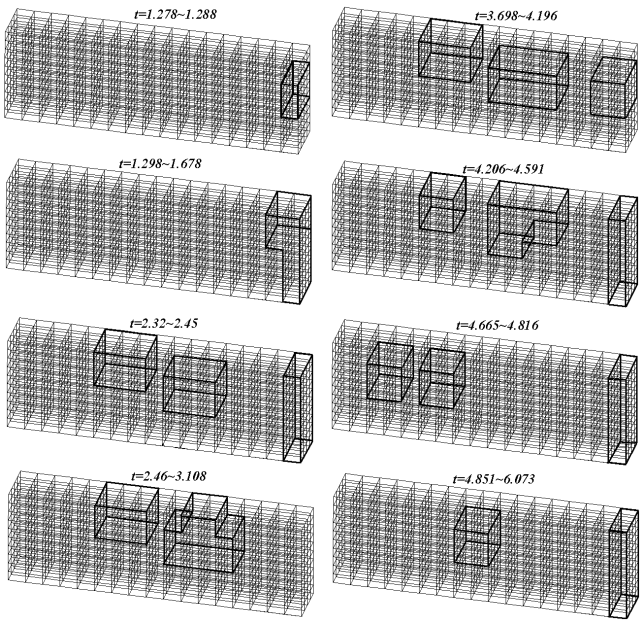

Fig. 16. development of cavitation in the Konya Dam reservoir in the first six second of the horizontal component of El-Centor earthquake

Fig. 16. Maximum and Minimum values of σ_{xx} due to dynamic response of Koyna gravity dam to El-Centro ground motion (Peak acceleration scaled to 1.0 g)

	σ_x at the center of the element (b)		σ_x at the center of the element (a)	
	Without cavitation	With cavitation	Without cavitation	With cavitation
Max. *(ton/m²)*	26.36	14.3	940.1	514.75
Min. *(ton/m²)*	-40.91	-28.14	-863.4	-524.36

9.4. Example 4: Cavitation effects on dynamic response of the concrete arch dam

The interest in this example is directed towards application of proposed method for the evaluation of reservoir cavitation on seismic response of arch dams. The benchmark problem is morrow Point arch dam. Arch dams are built as assemblages of monoliths separated by vertical contraction joints. It is common practice in arch dams located in seismic active regions to have shear keys at contraction joints, which together with friction affect the transfer of shear between the monoliths. Shear keys can be either beveled or unbeveled and grouted or ungrouted. If shear keyed grouted ,the case that assumed in the present study, the arch dam body integrated and we can ignored the effect of opening and closing of contraction joints during seismic excitation. The Morrow Point arch dam located on the Gunnison River in southwest Colorado has a height of *142 m* and a crest length of *219 m*. A detailed model description of the Morrow Point dam can be found in [26-27]. Fig. 17 shows coarse and refined 3D Finite Element model of coupled system along with relevant dimensions. we use 160,8-node fluid element in the model of reservoir and 80,20-node brick element for discretization of dam structure in coarse model and 912,8-node fluid element in the model of reservoir and 192,20-node brick element for discretization of dam structure in the refined mesh.

The same input excitation of example 2 is selected. In order to consider the effects of cavitation, the peak acceleration of the El Centro earthquake is amplified so that the maximum magnitude is of the order 1.0 g in the stream direction (x-direction). In the analysis, only the first 7 second of the earthquake is used. Proportional damping ratio in the first and sixth fundamental vibration modes of dam is assumed 5%. Similar to previous example in the present case we add 0.0015 fluid stiffness proportional artificial damping into fluid finite element formulation in order to eliminate spurious oscillation in numerical results and improve convergence of solution process. Arch dam response is analyzed and compared with each others using two finite element models of arch dam–reservoir system.

To clarify the response of the dam-reservoir system we depict Hydrodynamic pressure-time variation at two point of interface A and B, and displacement of the dam crest at point C and Stress-time Variation at the center of two element (a) and (b) these nodal points and elements are shown in Fig. 17.

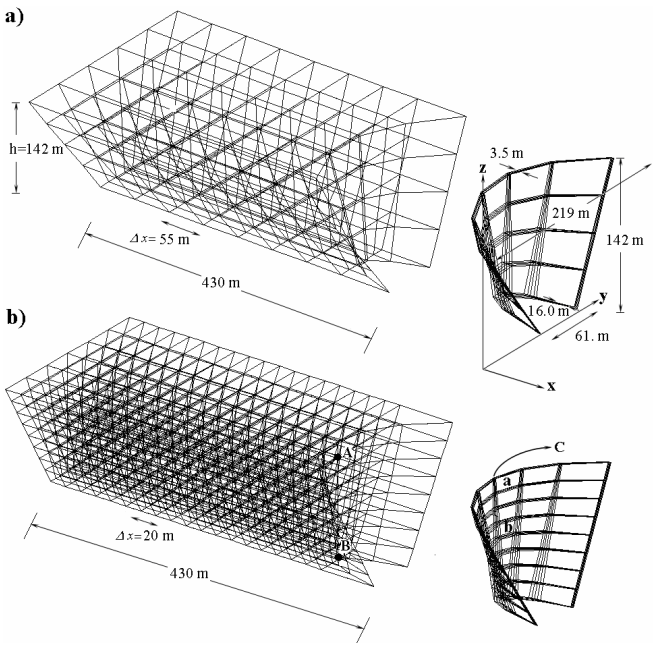

Fig. 17. Finite element model of morrow point arch dam with trapeze reservoir, a) coarse FE mesh, b) refined FE MESH.

Fig. 18, shows the response of morrow point arch dam to the first seven second of El-Centro earthquake, that excited the dam in upstream-downstream direction without amplification that evaluate using coarse and refined FE meshes.

The response of morrow point arch dam to the same earthquake that its peak acceleration scaled to *1.0 g* in order to truly modeled reservoir cavitation effects on seismic response of dam with using coarse and refined finite element mesh of the reservoir and dam domains, d are depict in Fig. 19 and Fig. 20, respectively. However, both models concluded similar results but with refining the FE mesh, we forced to add grater artificial damping into fluid domain to suppress numerical spurious oscillation.

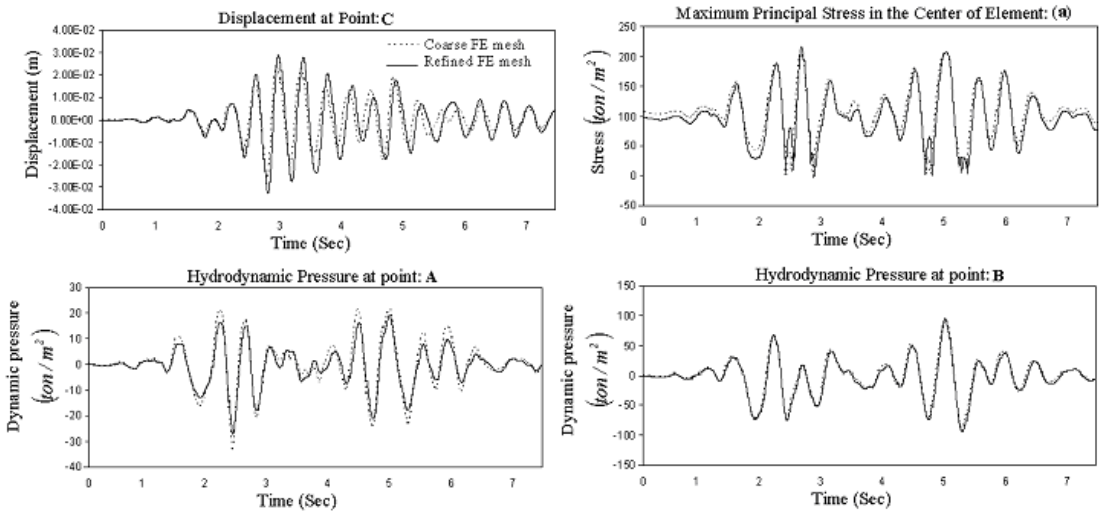

Fig. 18. Comparison of morrow point arch dam dynamic response subjected to horizontal component of El-centro earthquake for coarse and refined FE meshes

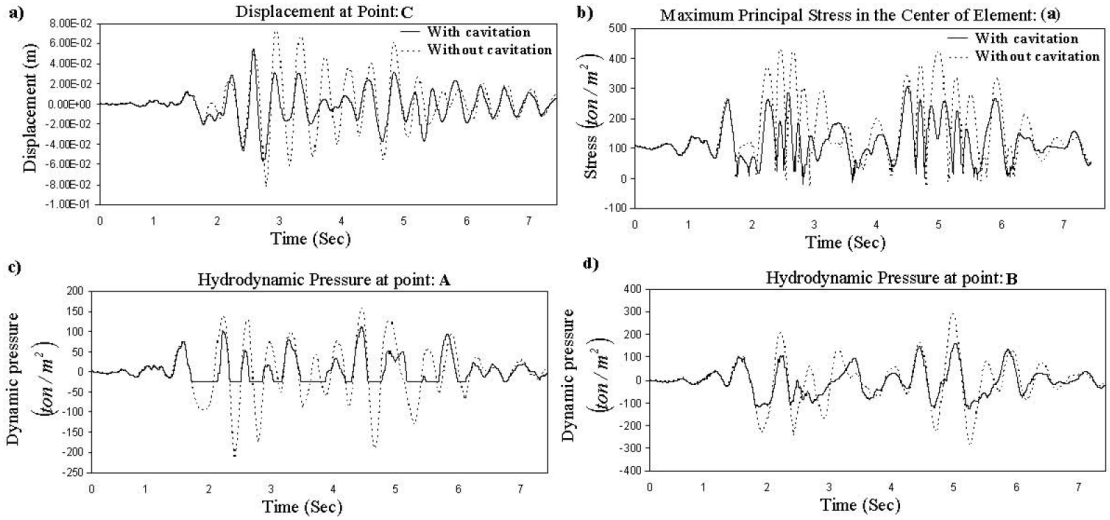

Fig. 19. Morrow point arch dam dynamic response due to horizontal component of El-centro earthquake with cavitation; peak acceleration scaled to 1.g. (Coarse FE mesh).

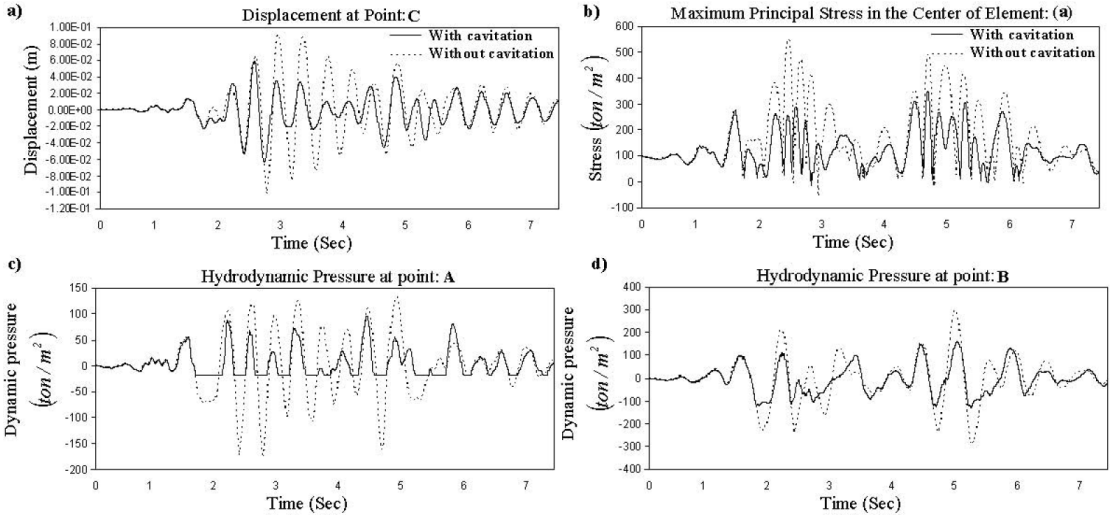

Fig. 20. Morrow point arch dam dynamic response due to horizontal component of El-Centro earthquake without cavitation effect; peak acceleration scaled to 1.g. (Refined FE mesh).

Comparison the results of analysis of arch dam with and without consideration of cavitation identify that a maximum crest displacement equal to *10.25 cm* with consideration of reservoir cavitation and 6.33 cm without cavitation at *t=2.62 sec*, that indicate *%38.2* decrease in the maximum crest displacement. Diversity between the results of analysis with and without consideration of reservoir cavitation on crest displacement begin at *t=1.80 Sec* and end at *t=5.25 Sec* time station that the cavitation effect decreases.

Maximum principal stress contour of arch dam is shown in Fig. 21, at three different time steps of analysis. However, cavitation cause considerable reduction in stress level in dam body, but some spike in stress is caused during collapsing cavitation regions in the reservoir, as shown in Fig. 21 (b).

The collapse of the cavitation regions when structure reverse direction, create larger peak pressures that if a linear fluid is assumed and cause larger displacement in the downstream direction. The maximum displacement in the upstream direction is generally reduced but in the present case the increased pressure associated with the collapse of the cavitated region of the fluid near the structure cause small increase in the upstream displacement. Ultimately, we can say cavitation effects on dynamic response of dam (displacement and stresses) are small.

10. Summary and Conclusions

A general time domain procedure using finite element technique has been presented for dynamic analysis of coupled dam-reservoir system including acoustic cavitation in the reservoir subjected to external excitations. The two different media, ie, the fluid and the solid region are solved individually and coupled effects are obtained through the proposed iterative scheme where equilibrium conditions along the common interface are satisfied. A desired level of convergence is achieved through a few numbers of iterations. At any instant of time *t*, a check was made for cavitated element in the fluid medium, if so exists cavitated fluid element, the stiffness of this element reduced then the fluid domain analysis again. This

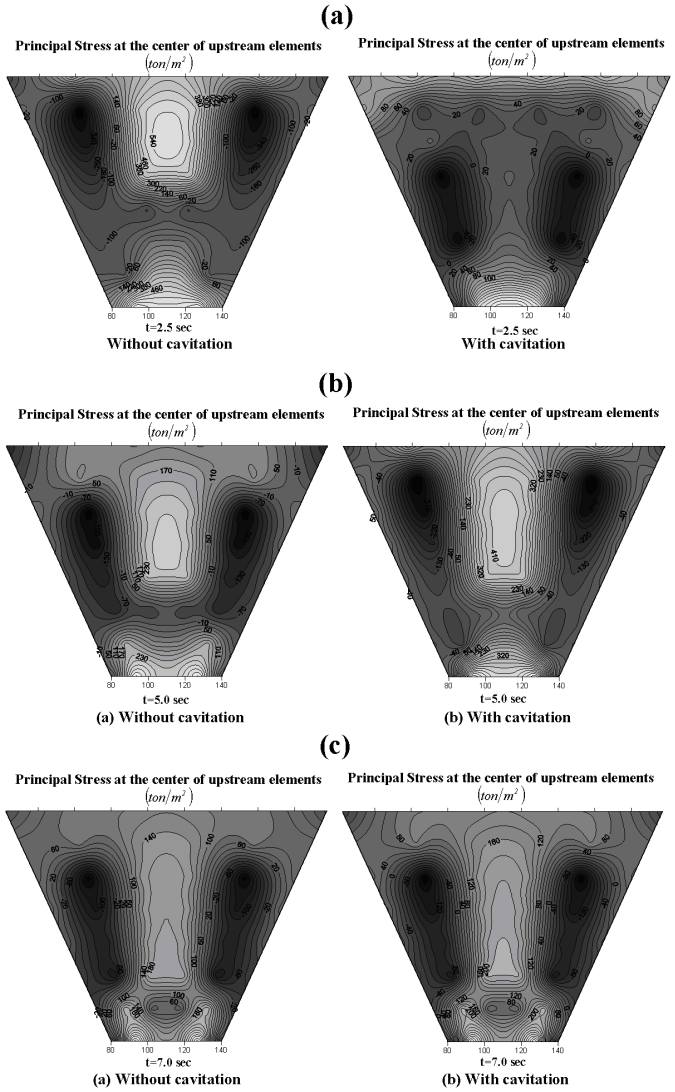

Fig. 21. Extremes of maximum principal stress due to dynamic response of Morrow Point arch dam to El-Centro ground motion (Peak acceleration scaled to 1.0 g)

process iterate until a desired level of convergence is achieved in fluid domain at the same time step. The major advantage of the proposed model are (a) the size of matrices required to be inverted is comparatively smaller as two systems are solved in a decoupled manner (b) Cavitaiton and induced impact forces can change the response of dam-reservoir system but its effects is small. (c) Cavitation inception depends on the magnitude of the peak earthquake acceleration that affects the dam-reservoir systems. In the present work, if no scale factor applies to El-Centro earthquake, cavitation does not occur in the reservoir. Therefore, we investigate a minimum amplified scale that required to cavitation forming in the reservoir, for a arch dam with 100 m height, a minimum scale factor equal with 1.154 and for a arch dam with 200 m height, a minimum scale factor equal with 1.124 required to cavitaition incept in the reservoir.

In order to further studies on seismic response of an arch dam one must consider a combination of opening-closing of contraction joints effects and nonlinear behavior of concrete along with nonlinear behavior of fluid due to cavitation that remains subject of further research.

References

[1] G. Fenves, L. M. Vargas-Loli, Nonlinear Dynamic Analysis of Fluid-Structure Systems. of Eng. Mechanics, Vol. [114].

[2] Kuhl, E., Hulshoff, S., De Borst, R., An arbitrary Lagrangian-Eulerian finite element approach for fluid-structure interaction phenomena, Int. J. for Numer. Meth. In Engng., 57,117-142, 2003.

[3] Koh, H. M., Kim, J. K., Park, J. H., Fluid-Structure interaction analysis of 3-D Rectangular tanks by a variationally coupled BEM-FEM and comparison with test Results. Earthquake Eng. Struct. Dyn., 27; 109-124, 1998.

[4] Niwa, A., and R. W. Clough. "Shaking Table Research on Concrete Dam Models." Report No. UCB/EERC-80/05. Earthquake Engineering Research Center, University of California, Berkeley. 1980.

[5] Clough, R. W., and Chang, C. H., Seismic cavitation effects on gravity dam Reservoir. , Numerical methods in coupled systems, R. W. Lewis, P. Bettess, and Hinton, eds., John Wiley and Sons, Chichester, UK. , 571-598. 1984

[6] H.H. Bleich and I. S. Sandler. Interaction between structures and bilinear fluids. International Journal of Solids and Structures, 6:617-639, 1970

[7] Zienkiewicz, O. C., and Paul, D. K., and Hinton, E., Cavitation in fluid-structure Response (with particular reference to dams under earthquake loading)., Earthquake Eng. Struct. Dyn. , 11(4), 463-481, 1983

[8] R. E. Newton. Finite element analysis of shock-induced cavitation. ASCE, Spring Convention, 1980. Preprint 80-110.

[9] Hamdi M. A. Ousset Y, Verchery G. A displacement method for the analysis of Vibrations of coupled fluid-structure systems. Int J Numer Meth Engng., 13, 139-50, 1978.

[10] C.A. Felippa and J.A. Deruntz, Finite element analysis of shock-induced hull Cavitiation, Computer Methods in Applied Mechanics and Engineering, 44:297–337, 1984.

[11] M.A. Sprague and T.L. Geers, Spectral elements and field separation for an Acoustic Fluid subject to cavitation, Journal of Computational Physics, 184:149– 162, 2003.

[12] G. Sandberg, A new finite element formulation of shock-induced hull cavitation, Comput. Methods Appl. Mech. Engng. 1995; 120:33-44

[13] M. R. Ross, M. A. Sprague, C. A. Felippa, K. C. Par, Treatment of acoustic fluid- structure interaction by localized Lagrange multipliers and comparison to alternative interface-coupling methods, Comput. Methods Appl. Mech. Engrg. 2009; 198:986-1005.

[14] D. Maity and S. K. Bhattacharyya. , Time Domain Analysis of infinite reservoir by Finit Element Method using a Novel Far-boundary Condition., Int. J. Finite Elements in Analysis and Design, 32; 85-96; 1999.

[15] Zienkiewicz, O. C. et al. The Sommerfeld radiation condition on infinite domains And its modeling in numerical procedure, IRIA Third Int. Symp. Comput. Meth Appl Sci Engng, 1977.

[16] S. Aliabadi and S. Tu and M. D. Watts, Simulation of Hydrodynamic Cavitating Flows Using Stabilized Finite Element Method, 43rd AIAA Aerospace Sciences Meeting & Exhibit, Jan. 10-13, 2005, Reno, Nevada

[17] A.V. Oskouei and A.A. Dumanoglu. Nonlinear dynamic response of concrete Gravity Dams: cavitation effect. Soil Dynamics and Earthquake Engineering, 21:99-112, 2001.

[18] N. Khalili, M. Yazdchi, and S. Valliappan. Non-linear seismic behavior of Concrete gravity dams using coupled finite element-boundary element technique. International Journal for Numerical Methods in Engineering, 44:101–130, 1999.

[19] Bahaa El-Aidi. Nonlinear Earthquake Response of Concrete Gravity Dam Systems. PhD Thesis, California Institute of Technology, Pasadena, 1989.

[20] H. Mirzabozorg and M. Ghaemian. Non-linear behavior of mass concrete in Three-dimensional problems using a smeared crack approach. Earth Engng and Struc. Dyn, 34:247-269, 2005

[21] O.C. Zienkiewicz and R.L. Taylor, the Finite Element Method: Basic Formulation And Linear Problems, volume 1, McGraw-Hill Book Company, London, Sixth Edition, 2004
[22] K.C. Park. Stabilization of partitioned solution procedures for pore fluid-soil Interaction analysis. Internat. J. Num. Meth. Eng., 19, 1669-73, 1983.
[23] M. Ghaemian and A. Ghobarah, Staggered Solution Schemes for Dam-Reservoir Interaction, J. of Fluids and Structures, 12, 933-948, 1998.
[24] M. R. Ross, "Coupling and Simulation of Acoustic Fluid-Structure Interaction Systems Using Localized Lagrange Multipliers",Ph.D. Thesis, Department of Aerospace Engineering Science, University of Colorado, 2006.
[25] Medina F. Modeling of soil-structure interaction by finite and infinite elements, Reports No. UCB/EERC-80/43, 1980.
[26] G. L. Fenves, S. Mojtahedi and R. B. Reimer, 'Effect of contraction joints On earthquake response of an arch dam, J. Struct. Engng. 118, 1039-1055 (1992).
[27] M. MAHMOOD R., M.T. Ahmadi, A. HAJMOMENI" AMBIENT VIBRATION TESTS OF A MODERUN ARCH DAM; SOME PROPOSALS FOR METHOD OF DATA PROCESSING", International J. of Civil Eng. Vol 1, Number 1 (9-2003).